

# Aero-Elastic Stability of Horizontal Axis Wind Turbine Blades

S. Sina

*Department of Mechanical and Mechatronics Engineering, Shahrood University of Technology, Shahrood, Iran.*

Received 22 June 2021; Revised Date 27 June 2021; Accepted Date 23 August 2021

\*Corresponding author: a.sina@shahroodut.ac.ir (S. Sina)

## Abstract

Multi-Megawatt wind turbines have long, slender, and heavy blades that can undergo extreme wind loadings. The aero-elastic stability of wind turbine blades is of great importance in both the power production and the load carrying capacity of structure. This paper investigates the aero-elastic stability of wind turbine blades modeled as thin-walled composite box beam utilizing unsteady incompressible aerodynamics. The structural model incorporates a number of non-classical effects such as the transverse shear, warping inhibition, non-uniform torsional model, and rotary inertia. The unsteady incompressible aerodynamics based on the Wagner's function is used in order to determine the aerodynamic loads. The governing differential equations of motion are obtained using the Hamilton's principle, and solved using the extended Galerkin's method. The results obtained are related to clarification of the effects of angular velocity and wind speed on the aero-elastic instability boundaries of the thin-walled composite beams. The results are expected to be useful toward obtaining better predictions of the aero-elastic behavior of composite rotating blades.

**Keywords:** *Wind Turbine Blade, Aero-elasticity, Unsteady Aerodynamic, Thin-Walled Composite Beam, Pre-twist Angle.*

## 1. Introduction

Aero-elasticity as the interaction between the inertial, elastic, and aerodynamic forces can have a significant effect on the wind turbine stability and life time. There exist a large amount of research works on the topic of wind turbine blade aero-elasticity. Wang et al. [1] have represented a detailed review on the aero-elastic modeling of wind turbine blades. A Thin-Walled Beam (TWB) is a slender structural element whose distinctive geometric dimensions are all of different orders of magnitude: its thickness is small compared to the cross-sectional dimensions, while its length greatly exceeds the dimensions of its cross-section. The theory of composite TWB was founded at first by Rehfield [2]. The state of the art in composite TWB was reviewed in a monograph by Librescu and Song [3]. Since the aircraft wing design is primarily based on the principle of TWBs, it is desirable to investigate the aero-elastic instability and aero-elastic response directly within the framework of thin-walled beams. To the best of the authors' knowledge, investigation of the flutter instability and dynamic aero-elastic response of advanced aircraft wings modeled as anisotropic thin-walled beams in subsonic flow appears to be rather scarce

in the open literature. Qin and Librescu [4] and Qin [5] have investigated the dynamic aero-elastic response of aircraft wings modeled as anisotropic thin-walled beams exposed to gust and blast loads. the solution of the aero-elastic system of governing equations requires a state-space description. Thus in the mentioned works, the unsteady aerodynamic loads are also converted into a state-space form. Shadmehri et al. [6] have extend the aero-elastic model to the case of aero-elastic analysis of wings with distance between the line of aerodynamic centers and the elastic axes of the wing.

In this work, which is an extension of the work reported in [6], an analytical model is developed in order to study the aero-elastic behavior of pre-twisted anisotropic rotating TWB. Based on the quasi polynomial approximation of the Wagner's function, the state space form of unsteady aerodynamics in time domain will be obtained, and then the Extended Galerkin Method (EGM) for spatial semi discretization will be applied to the governing aero-elastic equations. A set of numerical results is presented, and in addition, comparisons with a number of results in the literature are presented, and excellent agreements

are reported. The results obtained are expected to be useful toward obtaining better predictions of the aero-elastic instabilities of pre-twisted anisotropic rotating TWBs.

## 2. Equations of motion

### 2.1. Structural model

A pre-twisted composite TWB with length  $L$ , width  $c$ , height  $b$ , thickness  $h$ , and local pre-twist angle  $\beta(z)$  was considered, as shown in Figure 1. Besides the coordinates  $(x,y,z)$ , the local coordinates  $(x^p, y^p, z^p)$  were defined;  $x^p$  and  $y^p$  are the principal axes of the pre-twisted box beam cross-section. The  $z$ -axis was located so as to coincide with the locus of the symmetrical point of the box beam's cross-section along the beam span. The position vector  $\mathbf{R}$  of a point of deformed beam, measured from the edge of the beam, could be expressed as:

$$\begin{aligned} \mathbf{R} &= \mathbf{r} + \Delta, \mathbf{r} = x \vec{i} + y \vec{j} + z \vec{k} \\ \mathbf{R}_0 &= \mathbf{R}_0 \vec{k}, \Delta = u \vec{i} + v \vec{j} + w \vec{k} \end{aligned} \quad (1)$$

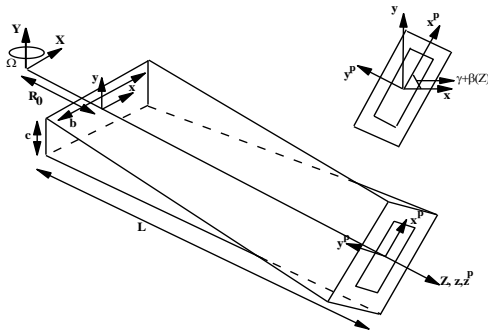


Figure 1. Structural model of a rotating pre-twisted TWB.

The displacement field is:

$$\begin{aligned} \mathbf{u} &= \mathbf{u}_0(\mathbf{z}, t) - \mathbf{y}\phi(\mathbf{z}, t), \mathbf{v} = \mathbf{v}_0(\mathbf{z}, t) + \mathbf{x}\phi(\mathbf{z}, t) \\ \mathbf{w} &= \mathbf{w}_0(\mathbf{z}, t) + (y - \mathbf{n} \, dx/ds) \theta_x(\mathbf{z}, t) + (x + \mathbf{n} \, dy/ds) \theta_y(\mathbf{z}, t) - \phi'(\mathbf{z}, t)(\mathbf{F}_w + \mathbf{n}a(s)) \end{aligned} \quad (2)$$

where  $u$ ,  $v$ , and  $w$  are the mid-surface displacements and  $\theta_x$ ,  $\theta_y$ ,  $\phi$  are the section normal vector rotations about the  $x$ -,  $y$ -, and  $z$ -directions, respectively;  $a(s)$ ,  $r(s)$ , and primary warping function ( $F_w$ ) are fully defined in [5]. In summary, substituting (2) in the linear strain-displacement relations and using the Hamilton's principle leads to the Euler-Lagrange equations and a set of natural and essential boundary conditions [6]. Using the constitutive relations for a general orthotropic material and assuming the symmetric angle-ply configuration, the Navier equations of motion could be expressed in terms of the displacement components, where there exists coupling between the vertical bending ( $\delta v$ ), twist

( $\delta\phi$ ), and transverse shear ( $\delta\theta_x$ ) equations of motion. The effects of pre-twist on the bending motions are applied using the simple transformation rules in order to transform the variables in local  $p$ -coordinate to the global coordinate [7] but pre-twist affects the torsion modes in different manners [8].

### 2.2. Aerodynamic model

By definition, an indicial function is the response to a disturbance that is applied instantaneously at time zero, and held constant thereafter, i.e. a disturbance is given by a step function. In the analysis of the flow about airfoil, if the indicial response to each kind of disturbances is known, then the unsteady loads to arbitrary changes in amount of any disturbances could be obtained through the superposition of indicial aerodynamic response using the Duhamel's integral. Wagner has obtained a solution for the indicial lift on a thin-airfoil undergoing a step change in the angle of attack in incompressible flow. In order to express the lift and aerodynamic moment in the state-space form, the quasi-polynomial approximation of the Wagner's function is used [9]. Finally, after amusing calculations, the aerodynamic loads could be expressed in the state space form [5].

## 3. Solution methodology

In order to convert the free vibration problem to an eigenvalue problem, the unknown variables  $F(\mathbf{z}, t)$  are written as:

$$\mathbf{F}(\mathbf{z}, t) = \tilde{\Psi}_F(\mathbf{z})\mathbf{q}(t) \quad (3)$$

Where  $\tilde{\Psi}_F(\mathbf{z})$  is the suitable assumed modes required to fulfill the geometric boundary conditions, and  $\mathbf{q}(t)$  is the vectors of generalized coordinates. Substituting (3) in the weak form of equations of motion, they are reduced to the following system of equations:

$$[\mathbf{M}]\{\dot{\mathbf{q}}\} + [\mathbf{C}]\{\dot{\mathbf{q}}\} + [\mathbf{K}]\{\mathbf{q}\} = \{\mathbf{0}\} \quad (4)$$

Where  $[\mathbf{M}]$ ,  $[\mathbf{C}]$ , and  $[\mathbf{K}]$  are the mass, damping, and stiffness matrices of the aero-elastic system, respectively. Re-writing (4) in the state space form and representing  $\mathbf{q}(t)$  in the form,  $\mathbf{q}(t) = \tilde{\mathbf{q}}\exp(\lambda t)$  leads to the eigenvalue form.

## 4. Numerical results

### 4.1. Validation

In order to verify the accuracy of the implemented structural model, a shearable cantilever pre-twisted beam is considered. In Table 1, two first

dimensionless natural frequencies ( $\bar{\omega}^2 = \omega^2 b_1 L^4 / a_{33}$ ) of beam are compared with those obtained from [18].

**Table 1. Comparison between natural frequencies of pre-twisted shearable beam of the present work and [18].**

	[18]	Present work
$\bar{\omega}_1$	3.516	3.515
$\bar{\omega}_2$	22.036	22.032
$a_{22} = 2869.7 \text{ N.m}^2, a_{33} = 57393 \text{ N.m}^2, b_1 = 34.47 \text{ kg/m},$ $L = 3.048 \text{ m}, \beta = 90$		

In order to verify the accuracy of the current solution methodology, the real and imaginary parts of the aero-elastic system for the wing model of Figure 2 with the parameters listed in Table 2 obtained in this work are compared with those obtained via the P-method. Figure 3(a) shows the damping of the aero-elastic modes obtained from the investigated solution methodology, while Figure 3(b) is obtained via the P-method. Figures 4 (a) and 4 (b) represent the variations in the frequencies of the aero-elastic system versus the free stream velocity obtained via the present and the P-method, respectively, which shows the accuracy of the solution methodology.

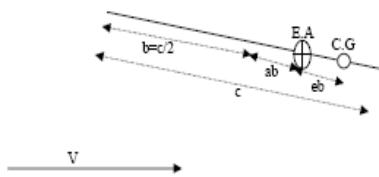


**Figure 2. A schematic description of the wing cross-section for solution methodology verification.**

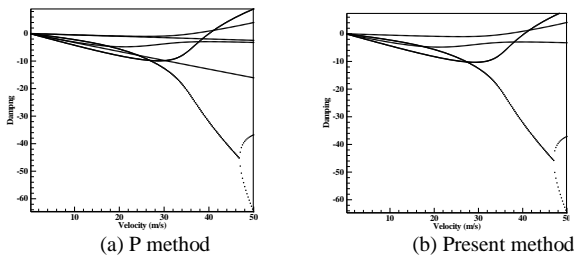


**Figure 3. Variation in dampings of aero-elastic system versus free stream velocity.**

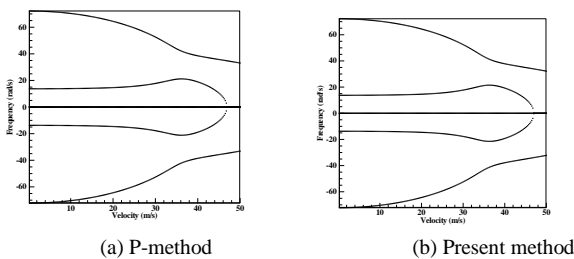


**Figure 4. Variation in the frequencies of aero-elastic system versus free stream velocity.**

**Table 2. Geometric specifications and material properties of the wing section for solution methodology verification.**

$X_a = e - a$	a	$m \text{ (kg)}$	$I_{c.g} \text{ (kgm}^2\text{)}$
0.4	-0.2	6.53	0.042
$EI \text{ (Nm}^2\text{)}$	$Gj \text{ (Nm}^2\text{)}$	$L \text{ (m)}$	$C \text{ (m)}$
159	1039	1	1.83

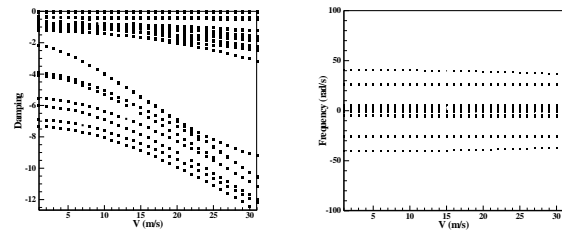
**4.2. Results**

The geometric and material properties of the studied blade are presented in Table 3.

**Table 2. Material and geometric properties of rotating composite TWB.**

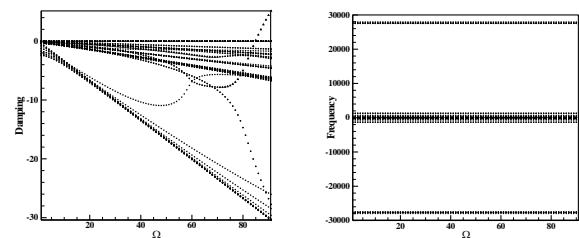
Geometric properties		Material properties	
L(m)	12	$E_1 \text{ (GPa)}$	206.8
b (m)	0.757	$E_2 = E_3 \text{ (GPa)}$	5.17
c (m)	0.1	$G_{12} = G_{13} \text{ (GPa)}$	3.1
h (m)	0.03	$G_{23} \text{ (GPa)}$	2.55
C (m)	0.9	Density $\text{(kg/m}^3\text{)}$	1528
		Poisson's ratio	0.3

Figure 5 shows the variation in the real and imaginary parts of the eigenvalues of the aero-elastic system versus wind velocity for  $\Omega = \Pi/3$ . The results obtained show that the effect of wind velocity on the aero-elastic system is marginal.



**Figure 5. Variation in the real and imaginary parts of eigenvalues of the aero-elastic system versus wind velocity for  $\Omega = \Pi/3$ .**

Figure 6 shows the effects of the rotational velocity on the real and imaginary parts of eigenvalues of the aero-elastic system.



**Figure 6. Variation in the real and imaginary parts of eigenvalues of the aero-elastic system versus rotational velocity.**

The flutter boundary of the blade is near the rotational velocity of 83 rad/s. A close look-up of the frequencies of the unstable aero-elastic modes is shown in Figure 7.

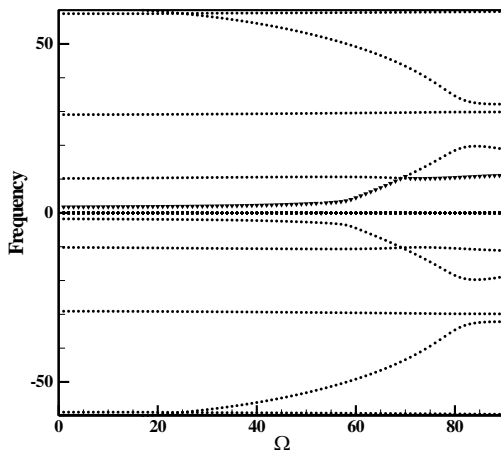


Figure 7. A close look-up of the frequencies of the unstable aero-elastic modes.

## 5. Conclusions

The aero-elastic stability of a horizontal axis wind turbine blade was investigated. The wind turbine blade structure was modeled as a rotating composite thin-walled beam. The structural model consists of the in-plane and out-of-plane bending, torsion, shear deformation, primary and secondary warping, rotary inertia, and warping inertia. The aerodynamic loads were obtained using the unsteady theory of aerodynamics and with polynomial representation of the corresponding lift deficiency function. The Eigen analysis of the aero-elastic system leads to the instability boundaries of the system. According the results of this work, the effect of the blade's rotational speed is dominant in comparison with the wind velocity on the occurrence of the flutter.

## 7. Acknowledgment

This article was presented in the 7<sup>th</sup> Iran Wind Energy Conference (IWEC 2021).

## References

[1] Corke T.C. and Thomas F.O., Dynamic Stall in Pitching Airfoils: Aerodynamic Damping and Compressibility Effects, *Annual Review of Fluid Mechanics*, Vol. 47, 2015, pp. 479-505.

[2] Bendiksen O., Kielb R.E., and Hall K.C., *Turbomachinery aero-elasticity*, Encyclopedia of Aerospace Engineering, 2010.

[3] Sicard J. and Sirohi J., Modeling of the large torsional deformation of an extremely flexible rotor in hover, *AIAA journal*, Vol. 52, 2014, pp.1604-15.

[4] Ondra V. and Titurus B., Theoretical and experimental modal analysis of a beam-tendon system. *Mechanical Systems and Signal Processing*, Vol. 132, 2019, pp. 55-71.

[5] Chen J., Shen X., Zhu X., and Du Z., Study on composite bend-twist coupled wind turbine blade for passive load mitigation, *Composite Structures*, Vol. 213, 2019, pp. 173-89.

[6] Librescu L., Song O., *Thin-walled Composite Beams: Theory and Application*, Springer, 2006, pp. 355.

[7] Houbolt J.C. and Brooks G.W., *Differential equations of motion for combined flapwise bending, chordwise bending, and torsion of twisted non-uniform rotating blades*, NASA TR 1346, 1958.

[8] Sicard J. and Sirohi, J., Modeling of the large torsional deformation of an extremely flexible rotor in hover, *AIAA journal*, Vol. 52, 2014, pp. 1604-15.

[9] Hodges D.H., *Non-linear composite beam theory*, American Institute of Aeronautics and Astronautics, 2006.

[10] Sapountzakis E.J. and Tsipiras, V.J., Shear deformable bars of doubly symmetrical cross-section under nonlinear non-uniform torsional vibrations—application to torsional post-buckling configurations and primary resonance excitations, *Nonlinear Dynamics*, Vol. 62, 2010, pp. 967-87.

[11] Sicard J.F. and Sirohi, J., An analytical investigation of the trapeze effect acting on a thin flexible ribbon, *Journal of Applied Mechanics*, Vol. 81, 2014.

[12] Mohri F., Meftah S.A., and Damil N., A large torsion beam finite element model for tapered thin-walled open cross-section beams, *Engineering Structures*, Vol. 99, 2015, pp.132-148.

[13] Han S. and Bauchau O.A., On the non-linear extension-twist coupling of beams, *European Journal of Mechanics-A/Solids*, Vol. 72, 2018, pp. 111-9.

[14] Nayfeh A.H. and Mook D.T., *Non-linear oscillations*, John Wiley and Sons; 2008.

[15] Sina S.A., Haddadpour H., and Navazi H.M., Non-linear free vibrations of thin-walled beams in torsion, *Acta Mechanica*, Vol. 223, 2012, pp: 2135-51.

[16] Sina S.A and Haddadpour H., Axial-torsional vibrations of rotating pre-twisted thin-walled composite beams, *International Journal of Mechanical Sciences*, Vol. 80, 2014, pp. 93-101.

[17] Sapountzakis E.J. and Tsipiras V.J., Non-linear non-uniform vibrations of bars by the boundary element method, *Journal of Sound and Vibration*, Vol. 329, No. 10, 2010, pp. 1853-1874.

[18] Haddadpour H., Kouchakzadeh M.A., and Shadmehry F., Aero-elastic Instability of Composite Aircraft Wings in an Incompressible Flow. *Composite Structures*. Vol. 38, 2008, pp. 93-99.